VEGF is essential for hypoxia-inducible factor-mediated neovascularization but dispensable for endothelial sprouting

Sunday Oladipupo[a,1], Song Hu[b,1], Joanna Kovalski[a], Junjie Yao[b], Andrea Santeford[a], Rebecca E. Sohn[a], Ralph Shohet[c], Konstantin Maslov[b], Lihong V. Wang[b,d,2], and Jeffrey M. Arbeit[a,d,2]

[a]Urology Division, Department of Surgery, and [c]Department of Medicine, University of Hawaii, 96813; and [b]Department of Biomedical Engineering and [d]Siteman Cancer Center, Washington University in St. Louis, 63110

Edited* by Gregg L. Semenza, The Johns Hopkins University School of Medicine, Baltimore, MD, and approved June 24, 2011 (received for review January 26, 2011)

Although our understanding of the molecular regulation of adult neovascularization has advanced tremendously, vascular-targeted therapies for tissue ischemia remain suboptimal. The master regulatory transcription factors of the hypoxia-inducible factor (HIF) family are attractive therapeutic targets because they coordinately up-regulate multiple genes controlling neovascularization. Here, we used an inducible model of epithelial HIF-1 activation, the TetON-HIF-1 mouse, to test the requirement for VEGF in HIF-1 mediated neovascularization. TetON-HIF-1, K14-Cre, and VEGF$^{flox/flox}$ alleles were combined to create TetON-HIF-1:VEGF$^{\Delta}$ mice to activate HIF-1 and its target genes in adult basal keratinocytes in the absence of concomitant VEGF. HIF-1 induction failed to produce neovascularization in TetON-HIF-1:VEGF$^{\Delta}$ mice despite robust up-regulation of multiple proangiogenic HIF targets, including PlGF, adrenomedullin, angiogenin, and PAI-1. In contrast, endothelial sprouting was preserved, enhanced, and more persistent, consistent with marked reduction in Dll4-Notch-1 signaling. Optical-resolution photoacoustic microscopy, which provides noninvasive, label-free, high resolution, and wide-field vascular imaging, revealed the absence of both capillary expansion and arteriovenous remodeling in serially imaged individual TetON-HIF-1:VEGF$^{\Delta}$ mice. Impaired TetON-HIF-1:VEGF$^{\Delta}$ neovascularization could be partially rescued by 12-*O*-tetradecanoylphorbol-13-acetate skin treatment. These data suggest that therapeutic angiogenesis for ischemic cardiovascular disease may require treatment with both HIF-1 and VEGF.

vascular biology | conditional expression | photoacoustic tomography | capillary imaging

Neovascularization is crucial for solid tumor growth and metastatic spread, for wound healing, and for tissue preservation and recovery after ischemia. Although tremendous progress has been made in understanding the molecular circuits regulating neovascularization in both benign and malignant disease, our knowledge remains incomplete. Solid tumors evade angiogenesis inhibitors, and efficacious therapeutic angiogenesis for tissue ischemia remains a tantalizing prospect.

The hypoxia-inducible factors-1 and -2 (HIF-1 and HIF-2) are αβ heterodimeric proteins that make crucial contributions to neovascularization in wound healing, and benign or malignant diseases (1, 2). HIFs are master regulatory transcription factors with >100 known, and potentially hundreds more, target genes containing the core RCGTG enhancer sequence (3–6). A collection of HIF target genes coordinates neovascularization at several levels including endothelial cell proliferation, microvessel tone, vascular remodeling, and proangiogenic myeloid cell recruitment (7).

Numerous reports suggested that HIF produced a more robust neovasculature, with more normal structure and function, compared with single angiogenic factor overexpression (2, 8–10). However, the contribution of individual target genes encoding vascular functions to the collective HIF-1 neovascular phenotype is unknown. Here, we tested the hypothesis that VEGF was dispensable for HIF-mediated neovascularization. We used a unique conditional model of adult neovascularization in the skin, the TetON-HIF-1 transgenic mouse (11) that displays multistage neovascularization, and myeloid cell recruitment and retention in the absence of disease. TetON-HIF-1 mice were engineered for germ-line Cre-mediated VEGF deletion in the same basal keratinocytes targeted for conditional adult HIF-1α induction. VEGF deletion abrogated neovascularization despite coordinate up-regulation of multiple angiogenic growth factors. Surprisingly, endothelial sprouting was activated after HIF-1 induction; however, these sprouts were nonproductive for neovessel development. Despite robust PlGF, adrenomedullin, and PAI-1 induction, HIF-1 activation in the absence of VEGF failed to affect vascular remodeling, and myeloid cell recruitment was markedly impaired. Thus, we provide evidence that VEGF is required for HIF-1–mediated adult neovascularization, but that certain elements of the angiogenic response proceed without this factor.

Results

TetON-HIF-1:VEGF$^{\Delta}$ Mice Lack Angiogenesis and Vessel Remodeling. To test the role of VEGF during epithelial HIF-1–induced neovascularization, we combined TetON-HIF-1 mice (11) with K14-Cre transgenic and VEGF floxed (VEGF$^{f/f}$) knock-in mice (12–15). The final genotype of these composite mice was K14-rtTA:TRE-HIF-1α$^{P402A/P564A/N803A}$:K14-Cre:VEGF$^{f/f}$. This genotype, designated as TetON-HIF-1:VEGF$^{\Delta}$, was $n = 12$ in the FVB/n strain. Doxycycline (DOX) treatment of 8- to 12-wk-old TetON-HIF-1:VEGF$^{f/f}$ mice induced a robust neovascularization that peaked and plateaued 14 d after initiation (Fig. 1 *A* and *B*). In contrast, neovascularization failed to occur in TetON-HIF-1:VEGF$^{\Delta}$ composite mice (Fig. 1 *A* and *B*). Moreover, contrary to prior reports (16), there was no reduction of microvascular density in TetON-HIF-1:VEGF$^{\Delta}$ composite mice, at baseline before DOX induction compared with nontransgenic controls, likely due to differences in tissue fixation/epitope preservation techniques and endothelial marker antibody detection reagents. Induction of HIF-1α protein expression was detectable in both interfollicular epidermal and hair follicle outer root sheath basal keratinocytes in both TetON-HIF-1:VEGF$^{\Delta}$ and TetON-HIF-1:VEGF$^{f/f}$ mice after 14 days of DOX induction (Fig. 1*C*).

Temporal control of HIF-1 allowed us to deploy an emerging technology for noninvasive and label-free functional determination of microvascular dynamics, optical-resolution photo-

Author contributions: S.O., S.H., K.M., L.V.W., and J.M.A. designed research; S.O., S.H., J.K., A.S., and R.E.S. performed research; R.S. and K.M. contributed new reagents/analytic tools; S.O., S.H., J.K., J.Y., L.V.W., and J.M.A. analyzed data; and S.O., S.H., J.Y., L.V.W., and J.M.A. wrote the paper.

Conflict of interest statement: L.V.W. has financial interest in Microphotoacoustics, Inc., and Endra, Inc., which, however, did not support this work. Other authors declare no competing financial interest.

*This Direct Submission article had a prearranged editor.

[1]S.O. and S.H. contributed equally to this work.

[2]To whom correspondence may be addressed. E-mail: arbeitj@wudosis.wustl.edu or lhwang@biomed.wustl.edu.

This article contains supporting information online at www.pnas.org/lookup/suppl/doi:10.1073/pnas.1101321108/-/DCSupplemental.

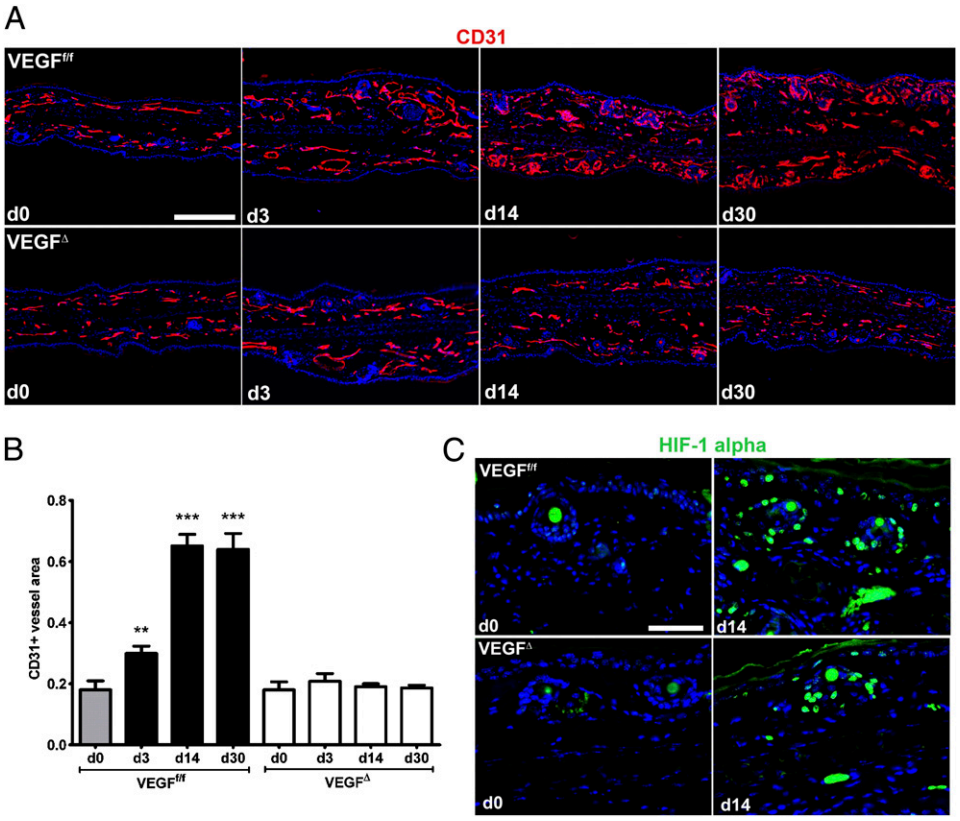

Fig. 1. Cre-mediated basal keratinocyte VEGF deletion abrogated HIF-1–induced neovascularization. (*A*) CD31 immunofluorescence (red) revealed robust neovascularization in TetON-HIF-1:VEGF$^{f/f}$ (VEGF$^{f/f}$) compared with TetON-HIF-1:VEGF$^{\Delta}$ (VEGF$^{\Delta}$) mice, which remained similar to baseline controls. DAPI was used as a nuclear counterstain. (*B*) Quantitative analysis of CD31+ vascular area revealed a threefold elevation in TetON-HIF-1:VEGF$^{f/f}$ compared with TetON-HIF-1:VEGF$^{\Delta}$ mice induced with doxycycline for similar time intervals (n = 3–6 mice per time point). (*C*) Representative HIF-1α transgene immunofluorescence indicating localization to the epidermal and hair follicle basal cell compartment after 14 d of DOX induction. (*B*) VEGF$^{\Delta}$ or VEGF$^{f/f}$ data at each DOX day were compared with VEGF$^{f/f}$ day 0 data by using the unpaired Student's t test (**P < 0.01 and ***P < 0.001). (Scale bars: *A*, 200 μm: *C*, 50 μm.)

acoustic microscopy (OR-PAM) (17, 18). The resolving power and image segmentation capabilities of OR-PAM enabled multiparameter determination of vascular morphology including capillary volume as an indicator of angiogenesis, and arteriovenous (arteriolar/venular) volume, vessel length, diameter, and tortuosity as measures of vascular remodeling. Because OR-PAM uses hemoglobin for contrast (17), both the imaging and quantitative segmentation analysis were based on perfused vessels, which, similar to ante mortem lectin perfusion (10), is distinct from data derived from endothelial marker analysis of postmortem tissue sections. Serial OR-PAM monitoring of individual mice from days 0 to 60 of continuous DOX provision revealed that HIF-1 activation in TetON-HIF-1:VEGF$^{f/f}$ mice produced an eightfold increase in capillary volume and a 3.5-fold elevation of arteriovenous and overall vascular volume compared with DOX-induced TetON-HIF-1:VEGF$^{\Delta}$ or day 0 TetON-HIF-1:VEGF$^{f/f}$ controls (Fig. 2*A* and Fig. S1*B*). OR-PAM segmentation analysis suggested that capillary volume fell between days 14 and 30 in the TetON-HIF-1:VEGF$^{f/f}$ mice (Fig. S1). The difference between these data and the microvessel density analysis based on CD31 decoration of all vessels could be due to the lack of perfusion of CD31-positive vessels or that OR-PAM acquires wide field volumetric data and immunofluorescence analyzes microvascular area in 2D tissue sections. OR-PAM also demonstrated abrogation of HIF-1–mediated vasodilatation and tortuosity induction in the absence of epithelial VEGF (Fig. S1*B*).

Loss of HIF-1–Induced VEGF Produces Sprouting Without Endothelial Proliferation. An outstanding feature of the TetON-HIF-1 model is the ability to dissect discrete stages of neovascular network development and its maintenance due to temporal control of HIF-1 gain of function (11). Here, we tested the necessity of VEGF for HIF-1 induction of the earliest stages of neovascularization, endothelial sprouting, and proliferation. DOX-treated NTG and day 0 TetON-HIF-1:VEGF$^{f/f}$ mice were used interchangeably in all studies, because they were phenotypically and functionally similar. Endothelial proliferation remained at barely detectable levels after HIF-1 activation in TetON-HIF-1:VEGF$^{\Delta}$ mice, in contrast to a robust induction in TetON-HIF-1:VEGF$^{f/f}$ counterparts (Fig. S2*A*). Surprisingly, TetON-HIF-1:VEGF$^{\Delta}$ mice evidenced a prolonged interval of endothelial sprouting up to day 14 during HIF-1 induction (Fig. 3*A, Left* and Fig. S2*B*). In contrast, sprout elaboration in TetON-HIF-1:VEGF$^{f/f}$ was restricted to the immediate postinduction interval, markedly evident at DOX day 3, but nearly undetectable by DOX day 14 (Fig. 3*A, Left* and Fig. S2*B*). Sprouts were not detectable in NTG mice at any interval during DOX treatment (Fig. 3*A, Left* and Fig. S2*B*). Because Dll4-Notch1 activation regulates vascular sprouting, and is downstream of VEGF signaling via VEGFR2 and VEGFR3 (19–21), we interrogated mouse ear cross-sections for dual Dll4/CD31 coimmunofluorescence (Fig. 3*A, Right*). Endothelial Dll4 expression levels in TetON-HIF-1:VEGF$^{\Delta}$ mice were low and similar to those of their NTG counterparts up to 30 d of continuous HIF-1 induction (Fig. 3*A, Right*). In contrast, TetON-HIF-1:VEGF$^{f/f}$ mice evidenced marked endothelial Dll4 up-regulation after 14 d of HIF-1 induction (Fig. 3*, Right Middle*). We further explored Notch-1 signaling by determining the expression kinetics and localization of the Notch intracellular domain (NICD), the product of the gamma secretase-mediated receptor cleavage and the active transcriptional Notch component (22). The NICD was detectable in both the day 14 TetON-HIF-1:VEGF$^{f/f}$ endothelium and in basal keratinocytes (Fig. 3*B*, arrowheads). In contrast, the NICD was detectable only in a few basal keratinocytes of TetON-HIF-1:VEGF$^{\Delta}$ mice. The levels of Dll4 and the downstream Notch target Hey 1 mRNA were elevated 7- to 10-fold in TetON-HIF-1:VEGF$^{f/f}$ mice compared with 14-d DOX-treated NTG controls (Fig. 3*C*). Dll4 and Hey-1 were induced at low, but statistically significant, levels in TetON-HIF-1:VEGF$^{\Delta}$ mice compared with NTG controls (Fig. 3*C*). Collectively, these data suggest that HIF-1 and its downstream targets (see below) are able to induce endothelial sprouting, yet these sprouts are nonproductive in forming neovessels in the absence of VEGF. The paucity of epidermal NICD in the TetON-HIF-1:VEGF$^{\Delta}$ mice demonstrates that VEGF is re-

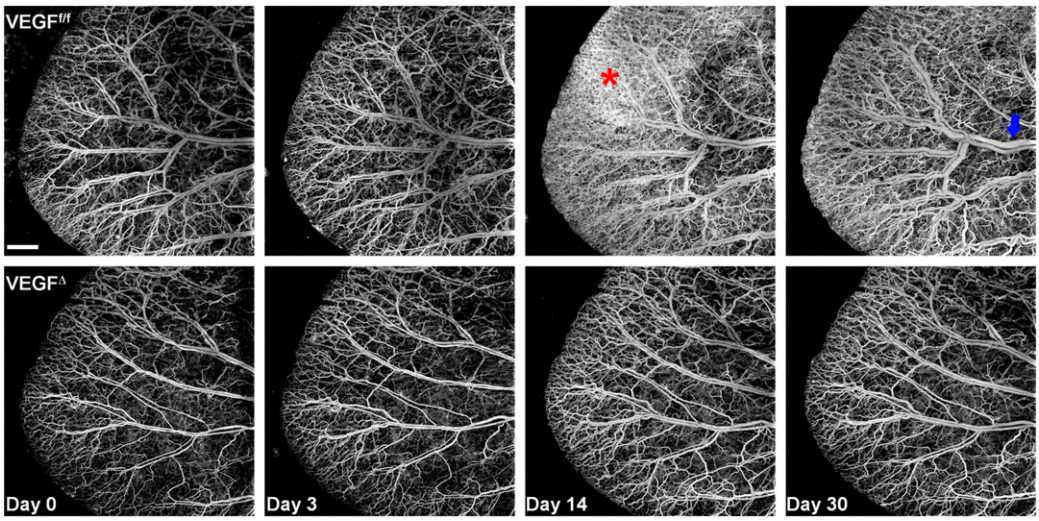

Fig. 2. TetON-HIF-1:VEGF$^{\Delta}$ mice lacked vessel remodeling. (*A*) Angiogenesis determination and accompanying vascular remodeling by OR-PAM. OR-PAM was performed in the same VEGF$^{f/f}$ or VEGF$^{\Delta}$ transgenic mouse serially for 60 d (days 0–30 are represented). Increased capillary density (red asterisk) is evident particularly by day 14, whereas arteriovenous remodeling (increase in vessel diameter and tortuosity) is detectable at day 14 and prominent by day 30 (blue arrow) (see also Fig. S1). (Scale bar: 500 μm.)

quired for robust Notch activation in this cellular tissue compartment after HIF-1 induction.

Induction of Multiple HIF-1 Angiogenic Target Genes Is Insufficient for Angiogenesis in the Absence of VEGF. Previous work has highlighted the angiogenic potential of several direct and indirect HIF-1 transcriptional targets (23–29). To determine whether these targets were induced by HIF-1 in the absence of VEGF, whole skin extracts were analyzed by using RT-PCR, ELISA, or antibody microarrays (Fig. 4 *A* and *E*). First, we determined the functional efficiency of keratin-14 regulated Cre-mediated VEGF deletion. Both mRNA and whole tissue ELISA revealed baseline or even lower VEGF levels, compared with DOX-treated NTG controls, despite HIF-1 induction.

Other targets exhibited four expression patterns. PIGF, angiogenin, MMP-9, PAI-1, and MMP-3 were up-regulated in TetON-HIF-1:VEGF$^{\Delta}$ mice at levels comparable with TetON-HIF-1:VEGF$^{f/f}$ controls (Fig. 4*F* and Fig. S3 *A* and *B*). Adrenomedullin (ADM) and iNOS expression were lower in TetON-HIF-1:VEGF$^{\Delta}$ mice on DOX day 3, increased during continuous HIF-1 activation for 14 and 30 d, yet did not reach the levels evident in TetON-HIF-1:VEGF$^{f/f}$ positive controls (Fig. 4 *B* and *C*). Carbonic anhydrase IX (CAIX) progressively increased in TetON-HIF-1:VEGF$^{\Delta}$ mice to levels comparable with TetON-HIF-1:VEGF$^{f/f}$ positive controls by 30 d of continuous HIF-1 induction (Fig. 4*D*). The fourth expression pattern tracked with VEGF expression, lack or markedly reduced induction in TetON-HIF-1:VEGF$^{\Delta}$ mice compared with marked up-regulation in TetON-HIF-1:VEGF$^{f/f}$ counterparts. These molecules, osteopontin (OPN), pentraxin-3 (PTX-3), cysteine-rich 61/connective tissue growth factor/nephroblastoma overexpressed (CCN3/NOV), and macrophage chemoattractant protein-1 (MCP-1), are expressed in activated inflammatory and stromal fibroblasts (30–32). Their expression pattern was consistent with the marked diminution in stromal myeloid cell recruitment and retention in TetON-HIF-1:VEGF$^{\Delta}$ compared with TetON-HIF-1:VEGF$^{f/f}$ mice (see below).

Epithelial VEGF Loss Markedly Impairs HIF-1–Mediated Myeloid Cell Recruitment. HIF-1 is known to induce myeloid cell mobilization, recruitment, and retention via VEGF, PlGF, and SDF1 (11, 33–36). As such, we determined myeloid cell recruitment to HIF-1 stimulated skin in the absence of concomitant VEGF. Surprisingly, there was no significant recruitment of CD45+, CD11b+, or F4/80+ myeloid, or mast cells in TetON-HIF-1:VEGF$^{\Delta}$ mice after 14 d of HIF-1 induction despite significant up-regulation of the VEGFR1 ligand, PlGF (Figs. 4*F* and 5 *A*–*C* and Fig. S4). By day 30, a significant increase in both CD45 and CD11b myeloid cells was achieved in TetON-HIF-1:VEGF$^{\Delta}$ mice; however, these myeloid cells were insufficient to facilitate neovascularization in the absence of epithelial VEGF (Fig. 5 *A*–*C* and Fig. S4). Myeloid cell infiltration after chronic HIF-1 gain of function in DOX day 30 TetON-HIF-1:VEGF$^{\Delta}$ mice was similar to our previous work with germ-line skin-targeted constitutive HIF-1 mutants in transgenic mice (37). There, stromal myeloid cell trafficking was regulated by chemokines not VEGF.

12-*O*-Tetradecanoylphorbol-13-Acetate (TPA)-Induced Inflammation Produces Extensive Vascular Remodeling with Minimal Microvascular Density Increase. Topical phorbol ester induces angiogenesis via enhanced VEGF secretion from the activated epithelium (38, 39). Single-dose TPA treatment produces transient skin changes resolving after 3–4 d in wild type mice. Previously, we discovered that germ-line K14-HIF-1$^{P402A/P564G}$ transgenic mice responded to single-dose TPA challenge with a marked and prolonged stromal and intraepithelial neutrophil infiltrate persisting for 3 wk (37). Neutrophil recruitment was secondary to HIF-1–enhanced NFκB signaling and NFκB chemokine target gene up-regulation by transgenic keratinocytes. We capitalized on this strategy to determine whether the lack of HIF-1–mediated neovascularization in TetON-HIF-1:VEGF$^{\Delta}$ vasculature could be rescued. TetON-HIF-1:VEGF$^{\Delta}$ and TetON-HIF-1:VEGF$^{f/f}$ were DOX-induced for 14 d to prime the keratinocytes and stroma and emulate germ-line constitutive activation. One dose of topical TPA was followed by ear harvest 10 d later. As reported, TPA treatment produced a marked recruitment and retention of CD45 stromal myeloid cells in TetON-HIF-1:VEGF$^{f/f}$ mice (37), without affecting the frequency of CD11b macrophages (Fig. S5 *A* and *B*). Both TPA-treated DOX day 14 TetON-HIF-1:VEGF$^{f/f}$ and TetON-HIF-1:VEGF$^{\Delta}$ mice ear epidermis was similarly punctuated by microabscesses filled with neutrophils (Fig. S6, *Right*), an observation consistent with our previous findings (37). Moreover, TPA did not further augment VEGF expression or neovascularization in TetON-HIF-1:VEGF$^{f/f}$ mice (Fig. 6 *A* and *B*). In contrast, single-dose TPA in TetON-HIF-1:VEGF$^{\Delta}$ mice produced a twofold increase in VEGF expression associated with a similar fold increase in neovessel area. TPA also produced a similar influx of neutrophils in TetON-HIF-1:VEGF$^{\Delta}$ mice (Fig. S5*A*, *Left* and *B, Upper*). Partial rescue of

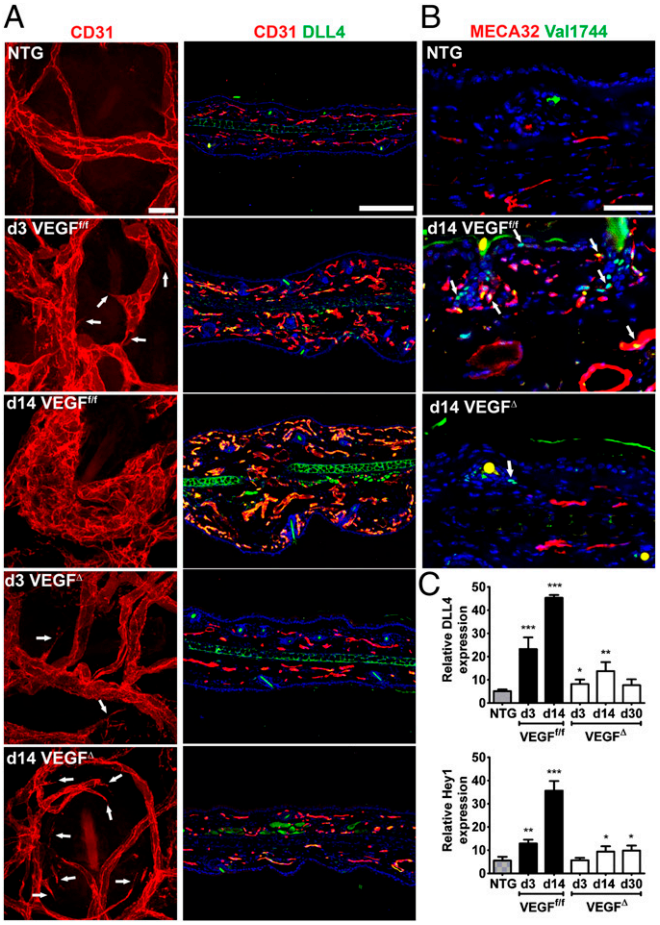

Fig. 3. Vessel sprouting increase with low-level increase of Notch activity in VEGF$^{\Delta}$ mice. (*A*) Representative confocal CD31 immunofluorescence showing vessel sprouting in TetON-HIF-1:VEGF$^{\Delta}$ and TetON-HIF-1VEGF$^{f/f}$ mice (arrows; *Left*). Note multiple sprouts in VEGF$^{\Delta}$ mice at DOX day 14 compared with their absence in VEGF$^{f/f}$ mice. Representative dual Dll4/CD31 immunofluorescence (*Right*). VEGF$^{f/f}$ mice showed marked endothelial Dll4 upregulation from 3 d of HIF-1 induction compared to VEGF δ mice and NTG counterparts. Sprouts were not detectable in DOX-treated NTG mice (*Left*). (*B*) Representative immunofluorescence of cleaved Notch1 intracellular domain (NICD, Val1744) in TetON-HIF-1:VEGF$^{\Delta}$ and TetON-HIF-1VEGF$^{f/f}$ mice (arrows; *Middle* and *Bottom*). (*C*) RT-PCR analysis (arbitrary units normalized to histone 3.3A) of the Notch1 ligand Dll4 and downstream target Hey1 showing marked 7- to 10-fold elevation in day 14 VEGF$^{f/f}$ mice (n = 3–4 mice per time point). In contrast, Dll4 and Hey-1 were induced at low, albeit statistically significant levels in VEGF$^{\Delta}$ mice. Data are mean ± SD. Statistical analysis was the unpaired Student t test comparing each VEGF$^{\Delta}$ or VEGF$^{f/f}$ DOX treatment day to comparably treated NTG controls: $*P < 0.05$, $**P < 0.01$ and $***P < 0.001$. (Scale bars: *A*, *Left*, 20 μm; *A*, *Right*, 200 μm; *B*, 50 μm.)

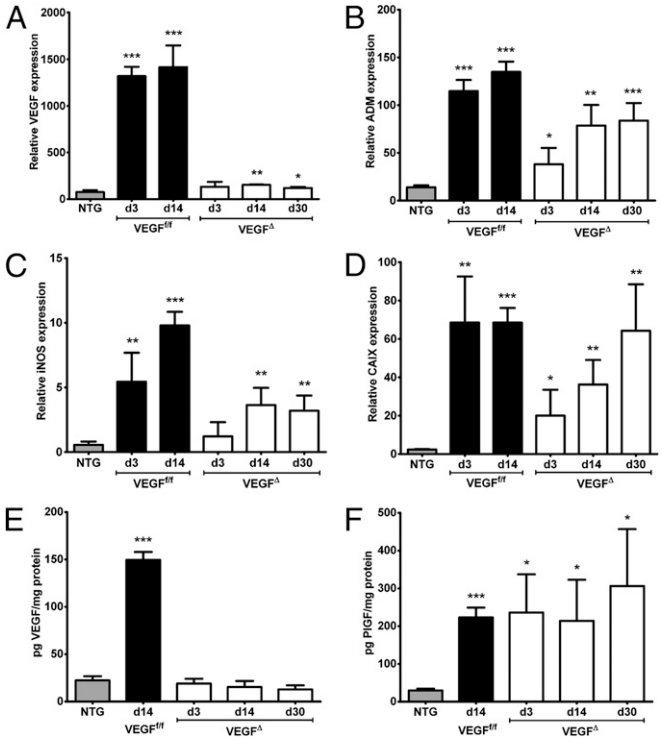

Fig. 4. Induction of multiple HIF-1 angiogenic targets in TetON-HIF-1:VEGF$^{\Delta}$ mice. (*A–D*) RT-PCR determination (arbitrary unit normalized against histone 3.3A) of differential patterns of HIF-1 target gene mRNA expression. Adrenomedullin (ADM) and iNOS increased 2.4-fold by day 3 in VEGF$^{\Delta}$ mice, but further increased by sevenfold during continuous HIF-1 induction for 14 and 30 d, yet did not reach the induction levels of VEGF$^{f/f}$ positive controls. Similarly, carbonic anhydrase IX (CAIX) progressively increased in VEGF$^{\Delta}$ mice to levels comparable to TetON-HIF-1:VEGF$^{f/f}$ positive controls by day 30 (n = 3–4 mice per time point). (*E*) Whole tissue ELISA revealed baseline or lower VEGF levels in VEGF$^{\Delta}$ mice, compared with DOX-treated NTG controls, during HIF-1 induction (n = 3 mice per time point). (*F*) PlGF was up-regulated in VEGF$^{\Delta}$ mice at similar levels as VEGF$^{f/f}$ controls (n = 3 mice per time point). Data analyzed as in Fig. 1: $*P < 0.05$, $**P < 0.01$, and $***P < 0.001$.

HIF-1–mediated neovascularization in TetON-HIF-1:VEGF$^{\Delta}$ mice was associated with expansion of an epidermal population of unrecombined VEGF$^{f/f}$ alleles and abscess-derived neutrophils (Fig. S5*B*). However, VEGF expression was undetectable in the majority of stromal neutrophils not associated with intraepidermal abcesses. TPA treatment also produced a statistically significant increase in capillary and total vessel volume, and a trend towards an increase in vessel tortuosity, as determined by OR-PAM (Fig. S7 *A* and *B*).

Discussion

In this study, we used a conditional mouse model to discover that VEGF, among a repertoire of induced angiogenic target genes, was necessary for HIF-1–mediated neovascularization. Targeting Tet-regulated HIF-1α to the skin had several advantages. We were able to use unfurred ear skin, enabling visual assessment of neovascular progression. The ear possessed a stereotypic histological architecture with a sharply delineated boundary between the transgene expressing basal keratinocytes and the underlying neovessel and inflammatory cell containing stroma. These features allowed us to determine alterations in tissue molecular signaling and immunofluorescent localization of induced signaling events covering the entire spectrum of neovascularization, from initial endothelial cell activation to development and maintenance of a complete neovascular network. This combination of tissue organization for molecular expression localization and immediate tissue sampling of an activated vasculature was distinct from disease models that required a lag phase to allow tumors to grow or ischemic neovascularization to become established. Other studies used adenoviral expression systems to create controlled time-dependent ear neovascularization (40). This approach had two challenges. First, there was an abrupt and massive overexpression of angiogenic factors followed by rapid decline. Second, viral particles were deposited in the stroma, an approach that did not model angiogenic signaling from an activated epithelium that, because it is initiated in the premalignant dysplasia, is an important component of multistage epithelial carcinogenesis (41).

As expected, we detected DOX-induced up-regulation of multiple angiogenic target genes that could have compensated for VEGF deficiency in TetON-HIF-1:VEGF$^{\Delta}$ mice. A lead example was the indirect HIF target PlGF. PlGF binds and activates VEGFR1 and induces phosphorylation of a repertoire of target

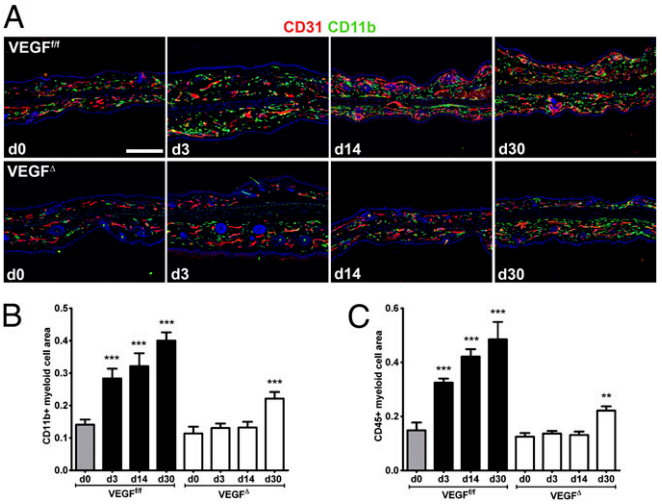

Fig. 5. HIF-1–mediated myeloid cell recruitment is abrogated in the absence of VEGF. (*A*) Representative CD31/CD11b coimmunofluorescence showing marked temporal delay and diminution of stromal myeloid cell infiltration in VEGF$^{\Delta}$ mice compared with early and robust CD11b+ myeloid cell recruitment inVEGF$^{f/f}$ counterparts. (*B* and *C*) Quantification of stromal area occupied by CD11b+ (*B*) (n = 3–4 mice per time point) and CD45+ cells (*C*; see Fig. S5 for representative immunofluorescent images) (n = 3–6 mice per time point). Data analyzed as in Fig. 1: *P < 0.05, **P < 0.01, and ***P < 0.001. (Scale bar: 200 μm.)

proteins distinct from VEGFR2 in endothelial cells (42, 43). PlGF has been shown to amplify or inhibit VEGF signaling through multiple mechanisms (44, 45). PlGF was angiogenic when targeted for overexpression in basal keratinocytes (23), or after local adenoviral injection in the skin or aortic adventitia (24, 25). PlGF gene deletion or antibodies targeting PlGF inhibited tumor growth via multiple mechanisms, including inhibition of angiogenesis, myeloid cell, and hematopoietic precursor mobilization (24, 35, 36). In models of tissue ischemia, PlGF was required for vascular dilatation and collateralization (24, 46). Thus, we were surprised that despite robust PlGF induction, angiogenesis, vascular dilatation, arteriovenous remodeling, and myeloid cell recruitment were unaffected by HIF-1 induction in the absence of VEGF. As such, our work is consistent with the VEGF signaling amplification function of PlGF, but is in contrast to "direct" angiogenesis induction of prior skin and adenoviral studies. The VEGF dominance in our model is also in line with recent studies questioning the contribution of PlGF to angiogenesis (47, 48).

In addition to PlGF, other angiogenic targets and vascular remodeling molecules were up-regulated in TetON-HIF-1:VEGF$^{\Delta}$ mice. The HIF target adrenomedullin was shown to promote physiological and pathological angiogenesis in vitro and in animal models (49–51). ADM signals angiogenesis by binding calcitonin-receptor-like receptor, which is widely expressed on normal and hypoxic endothelial cells (49, 52). Angiogenin was another molecule previously demonstrated to be angiogenic, yet without consequence in TetON-HIF-1:VEGF$^{\Delta}$ mice (28, 29). In addition to these direct proangiogenic HIF targets, molecules contributing accessory functions such as matrix degradation and its modulation, MMP9, MMP3, and PAI-1, and vascular dilatation, iNOS, were also up-regulated in TetON-HIF-1:VEGF$^{\Delta}$ mice. Thus, many of the molecules in the angiogenic "toolbox" were elevated by HIF-1, yet all required coordinate VEGF up-regulation to affect neovascularization and its modulation. Our data provide additional insight into studies wherein deletion of the VEGF HIF hypoxia response element (HRE) in ES cells or targeted germ-line VEGF gene deletion in keratinocytes diminished tumor growth (53) or delayed normal wound healing (16), respectively. However, in each of these studies, variable levels of neovascularization were present, likely from compensatory angiogenic factors. Our use of topical TPA challenge with its attendant prolonged stromal inflammation and neovascularization rescue emulated disease-associated angiogenic compensation. We were surprised that the VEGF increment induced by TPA in TetON-HIF-1:VEGF$^{\Delta}$ mice was not due to the numerous neutrophils infiltrating throughout the stroma. Rather, the VEGF increment was localized to the epidermis, likely due to expansion of a small population of preexisting basal keratinocytes with unrecombined VEGF$^{f/f}$ alleles and to focal neutrophil accumulations beneath intraepidermal abscesses. These data did not rule out a neovessel activation function for the stromal neutrophils, which have been shown in previous studies to be sources of compensatory angiogenic factors such as FGF-2 in tumors during VEGF signaling blockade (54). As such, our conditional model enabled precise genetic dissection of "intrinsic" HIF-1 functions while enabling titration of pathophysiological processes to test for complementation of baseline neovascularization deficiencies.

Finally, ear skin allowed us to continue to use an emerging technique for determination of neovascular architecture and microvessel function photoacoustic microscopy (PAM) (17). PAM and the derivative used in our study, OR-PAM, use red blood cell (RBC) hemoglobin for endogenous contrast. Diffraction-limited optical focusing and exquisite (100%) sensitivity to optical absorption enables single RBC resolution and capillary resolution in vivo (18). Additionally, the wide field of view of OR-PAM enabled us to determine the necessity of VEGF for both angiogenesis and arteriovenous remodeling in the context of HIF-1 induction. These features plus simultaneous determination of multiple parameters of neovascular function and tissue metabolism will be a boon for future studies in models of neovascular disease (17).

In conclusion, we demonstrate that despite induction of multiple angiogenic target genes, VEGF is necessary for HIF-1 mediated neovascularization. The VEGF requirement can be substantially, although not entirely, rescued by chemokine-activated keratinocytes and neutrophils accumulating adjacent to abscesses. Recent studies have demonstrated provocative linkage between age, cardiovascular disease, and insufficiency of HIF-1 expression in both ischemic tissues and infiltrating myeloid cells (55, 56). Because aging can also impair induction of VEGF expression (57, 58), our work suggests that therapeutic angiogenesis may require combinatorial restoration or administration of both HIF-1 and VEGF to achieve optimal tissue neovascularization.

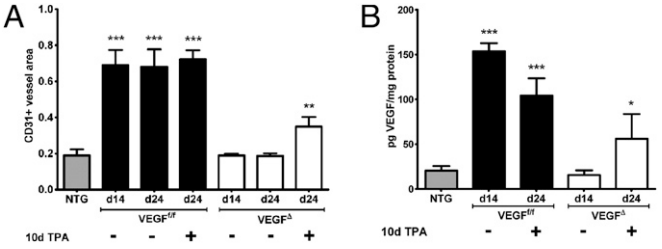

Fig. 6. 12-*O*-Tetradecanoylphorbol-13-acetate (TPA) treatment partially rescues neovascularization and results in moderate VEGF induction. (*A*) Quantification of CD31(+) area in (n = 3–6 mice per time point) revealed a twofold increase in neovascularization in TPA-treated VEGF$^{\Delta}$ mice. (*B*) Whole ear tissue ELISA for VEGF. A single dose of TPA in VEGF$^{\Delta}$ mice produced a twofold increase in VEGF. In contrast, VEGF levels were not further increased in TPA-treated VEGF$^{f/f}$ mice. (n = 3–6 mice per time point). Data analyzed as in Fig. 1: *P < 0.05, **P < 0.01, and ***P < 0.001.

Materials and Methods

Mouse Development, Target Expression Analysis, Photoacoustic Microscopy, and Inflammation Challenge. Detailed description of the mouse intercrosses to generate target and control genotypes, tissue molecular and expression analysis, photoacoustic microscopy, and inflammation challenge experiments are available in *SI Materials and Methods*. The Animal Studies Committee of Washington University in St. Louis approved all animal care and experimental procedures.

Statistical Analysis. The data are reported as the mean ± SD. Data from DOX-treated TetON-HIF-1:VEGF$^{\Delta}$ or TetON-HIF-1VEGF$^{f/f}$ mice were compared either with day 0 or NTG mice treated with DOX for the same interval by using the unpaired Student *t* test (GraphPad Prism 5). There were 3–6 mice per group unless otherwise indicated.

ACKNOWLEDGMENTS. We thank Hans Peter Gerber and Napoleon Ferrara for the gift of the VEGF$^{flox/flox}$ mice, Rick Bruick for the gift of the TRE-HIF-1$\alpha^{P402A/P464A/N803A}$ plasmid for construction of the TRE-HIF-1$\alpha^{P402/464A/N803A}$ transgenic mice, and Adam Glick for the gift of the K5-rtTA transgenic mice. This work was supported by National Institutes of Health Grants R01-CA90722, R01 EB000712, R01 NS46214, R01 EB008085, and U54 CA136398, and the Beatrice Roe Urologic Cancer Fund.

1. Hickey MM, Simon MC (2006) Regulation of angiogenesis by hypoxia and hypoxia-inducible factors. *Curr Top Dev Biol* 76:217–257.
2. Rey S, Semenza GL (2010) Hypoxia-inducible factor-1-dependent mechanisms of vascularization and vascular remodelling. *Cardiovasc Res* 86:236–242.
3. Wenger RH, Stiehl DP, Camenisch G (2005) Integration of oxygen signaling at the consensus HRE. *Sci STKE* 2005:re12.
4. Ortiz-Barahona A, Villar D, Pescador N, Amigo J, del Peso L (2010) Genome-wide identification of hypoxia-inducible factor binding sites and target genes by a probabilistic model integrating transcription-profiling data and in silico binding site prediction. *Nucleic Acids Res* 38:2332–2345.
5. Mole DR, et al. (2009) Genome-wide association of hypoxia-inducible factor (HIF)-1alpha and HIF-2alpha DNA binding with expression profiling of hypoxia-inducible transcripts. *J Biol Chem* 284:16767–16775.
6. Benita Y, et al. (2009) An integrative genomics approach identifies Hypoxia Inducible Factor-1 (HIF-1)-target genes that form the core response to hypoxia. *Nucleic Acids Res* 37:4587–4602.
7. Semenza GL (2010) Vascular responses to hypoxia and ischemia. *Arterioscler Thromb Vasc Biol* 30:648.
8. Kelly BD, et al. (2003) Cell type-specific regulation of angiogenic growth factor gene expression and induction of angiogenesis in nonischemic tissue by a constitutively active form of hypoxia-inducible factor 1. *Circ Res* 93:1074–1081.
9. Hirota K, Semenza GL (2006) Regulation of angiogenesis by hypoxia-inducible factor 1. *Crit Rev Oncol Hematol* 59:15–26.
10. Elson DA, et al. (2001) Induction of hypervascularity without leakage or inflammation in transgenic mice overexpressing hypoxia-inducible factor-1alpha. *Genes Dev* 15: 2520–2532.
11. Oladipupo SS, et al. (2011) Conditional HIF-1 induction produces multistage neovascularization with stage-specific sensitivity to VEGFR inhibitors and myeloid cell independence. *Blood* 117:4142–4153.
12. Bekeredjian R, et al. (2010) Conditional HIF-1alpha expression produces a reversible cardiomyopathy. *PLoS ONE* 5:e11693.
13. Diamond I, Owolabi T, Marco M, Lam C, Glick A (2000) Conditional gene expression in the epidermis of transgenic mice using the tetracycline-regulated transactivators tTA and rTA linked to the keratin 5 promoter. *J Invest Dermatol* 115:788–794.
14. Jonkers J, et al. (2001) Synergistic tumor suppressor activity of BRCA2 and p53 in a conditional mouse model for breast cancer. *Nat Genet* 29:418–425.
15. Gerber HP, et al. (1999) VEGF is required for growth and survival in neonatal mice. *Development* 126:1149–1159.
16. Rossiter H, et al. (2004) Loss of vascular endothelial growth factor a activity in murine epidermal keratinocytes delays wound healing and inhibits tumor formation. *Cancer Res* 64:3508–3516.
17. Wang LV (2009) Multiscale photoacoustic microscopy and computed tomography. *Nat Photonics* 3:503–509.
18. Maslov K, Zhang HF, Hu S, Wang LV (2008) Optical-resolution photoacoustic microscopy for in vivo imaging of single capillaries. *Opt Lett* 33:929–931.
19. Tammela T, et al. (2008) Blocking VEGFR-3 suppresses angiogenic sprouting and vascular network formation. *Nature* 454:656–660.
20. Thurston G, Noguera-Troise I, Yancopoulos GD (2007) The Delta paradox: DLL4 blockade leads to more tumour vessels but less tumour growth. *Nat Rev Cancer* 7:327–331.
21. Hellström M, et al. (2007) Dll4 signalling through Notch1 regulates formation of tip cells during angiogenesis. *Nature* 445:776–780.
22. Kopan R, Ilagan MXG (2009) The canonical Notch signaling pathway: Unfolding the activation mechanism. *Cell* 137:216–233.
23. Odorisio T, et al. (2002) Mice overexpressing placenta growth factor exhibit increased vascularization and vessel permeability. *J Cell Sci* 115:2559–2567.
24. Luttun A, et al. (2002) Revascularization of ischemic tissues by PlGF treatment, and inhibition of tumor angiogenesis, arthritis and atherosclerosis by anti-Flt1. *Nat Med* 8:831–840.
25. Roy H, et al. (2005) Adenovirus-mediated gene transfer of placental growth factor to perivascular tissue induces angiogenesis via upregulation of the expression of endogenous vascular endothelial growth factor-A. *Hum Gene Ther* 16:1422–1428.
26. Abe M, et al. (2003) Adrenomedullin augments collateral development in response to acute ischemia. *Biochem Biophys Res Commun* 306:10–15.
27. Oehler MK, Hague S, Rees MC, Bicknell R (2002) Adrenomedullin promotes formation of xenografted endometrial tumors by stimulation of autocrine growth and angiogenesis. *Oncogene* 21:2815–2821.
28. Raghu H, et al. (2010) Suppression of uPA and uPAR attenuates angiogenin mediated angiogenesis in endothelial and glioblastoma cell lines. *PLoS ONE* 5:e12458.
29. Yoshioka N, Wang L, Kishimoto K, Tsuji T, Hu GF (2006) A therapeutic target for prostate cancer based on angiogenin-stimulated angiogenesis and cancer cell proliferation. *Proc Natl Acad Sci USA* 103:14519–14524.
30. Mantovani A, Garlanda C, Doni A, Bottazzi B (2008) Pentraxins in innate immunity: From C-reactive protein to the long pentraxin PTX3. *J Clin Immunol* 28:1–13.
31. Keeley EC, Mehrad B, Strieter RM (2008) Chemokines as mediators of neovascularization. *Arterioscler Thromb Vasc Biol* 28:1928–1936.
32. Scatena M, Liaw L, Giachelli CM (2007) Osteopontin: A multifunctional molecule regulating chronic inflammation and vascular disease. *Arterioscler Thromb Vasc Biol* 27:2302–2309.
33. Ceradini DJ, et al. (2004) Progenitor cell trafficking is regulated by hypoxic gradients through HIF-1 induction of SDF-1. *Nat Med* 10:858–864.
34. Grunewald M, et al. (2006) VEGF-induced adult neovascularization: Recruitment, retention, and role of accessory cells. *Cell* 124:175–189.
35. Hattori K, et al. (2002) Placental growth factor reconstitutes hematopoiesis by recruiting VEGFR1(+) stem cells from bone-marrow microenvironment. *Nat Med* 8: 841–849.
36. Fischer C, et al. (2007) Anti-PlGF inhibits growth of VEGF(R)-inhibitor-resistant tumors without affecting healthy vessels. *Cell* 131:463–475.
37. Scortegagna M, et al. (2008) HIF-1alpha regulates epithelial inflammation by cell autonomous NFkappaB activation and paracrine stromal remodeling. *Blood* 111: 3343–3354.
38. Kishimoto J, et al. (2000) In vivo detection of human vascular endothelial growth factor promoter activity in transgenic mouse skin. *Am J Pathol* 157:103–110.
39. Morris PB, Hida T, Blackshear PJ, Klintworth GK, Swain JL (1988) Tumor-promoting phorbol esters induce angiogenesis in vivo. *Am J Physiol* 254:C318–C322.
40. Nagy JA, Shih SC, Wong WH, Dvorak AM, Dvorak HF (2008) Chapter 3. The adenoviral vector angiogenesis/lymphangiogenesis assay. *Methods Enzymol* 444:43–64.
41. Hanahan D, Folkman J (1996) Patterns and emerging mechanisms of the angiogenic switch during tumorigenesis. *Cell* 86:353–364.
42. Park JE, Chen HH, Winer J, Houck KA, Ferrara N (1994) Placenta growth factor. Potentiation of vascular endothelial growth factor bioactivity, in vitro and in vivo, and high affinity binding to Flt-1 but not to Flk-1/KDR. *J Biol Chem* 269:25646–25654.
43. Landgren E, Schiller P, Cao Y, Claesson-Welsh L (1998) Placenta growth factor stimulates MAP kinase and mitogenicity but not phospholipase C-gamma and migration of endothelial cells expressing Flt 1. *Oncogene* 16:359–367.
44. Eriksson A, et al. (2002) Placenta growth factor-1 antagonizes VEGF-induced angiogenesis and tumor growth by the formation of functionally inactive PlGF-1/VEGF heterodimers. *Cancer Cell* 1:99–108.
45. Autiero M, et al. (2003) Role of PlGF in the intra- and intermolecular cross talk between the VEGF receptors Flt1 and Flk1. *Nat Med* 9:936–943.
46. Pipp F, et al. (2003) VEGFR-1-selective VEGF homologue PlGF is arteriogenic: Evidence for a monocyte-mediated mechanism. *Circ Res* 92:378–385.
47. Van de Veire S, et al. (2010) Further pharmacological and genetic evidence for the efficacy of PlGF inhibition in cancer and eye disease. *Cell* 141:178–190.
48. Bais C, et al. (2010) PlGF blockade does not inhibit angiogenesis during primary tumor growth. *Cell* 141:166–177.
49. Nikitenko LL, et al. (2006) Adrenomedullin and CGRP interact with endogenous calcitonin-receptor-like receptor in endothelial cells and induce its desensitisation by different mechanisms. *J Cell Sci* 119:910–922.
50. Ishikawa T, et al. (2003) Adrenomedullin antagonist suppresses in vivo growth of human pancreatic cancer cells in SCID mice by suppressing angiogenesis. *Oncogene* 22:1238–1242.
51. Shindo T, et al. (2001) Vascular abnormalities and elevated blood pressure in mice lacking adrenomedullin gene. *Circulation* 104:1964–1971.
52. Nikitenko LL, Smith DM, Bicknell R, Rees MC (2003) Transcriptional regulation of the CRLR gene in human microvascular endothelial cells by hypoxia. *FASEB J* 17: 1499–1501.
53. Tsuzuki Y, et al. (2000) Vascular endothelial growth factor (VEGF) modulation by targeting hypoxia-inducible factor-1alpha—> hypoxia response element—> VEGF cascade differentially regulates vascular response and growth rate in tumors. *Cancer Res* 60:6248–6252.
54. Casanovas O, Hicklin DJ, Bergers G, Hanahan D (2005) Drug resistance by evasion of antiangiogenic targeting of VEGF signaling in late-stage pancreatic islet tumors. *Cancer Cell* 8:299–309.
55. Bosch-Marce M, et al. (2007) Effects of aging and hypoxia-inducible factor-1 activity on angiogenic cell mobilization and recovery of perfusion after limb ischemia. *Circ Res* 101:1310–1318.
56. Rey S, et al. (2009) Synergistic effect of HIF-1alpha gene therapy and HIF-1-activated bone marrow-derived angiogenic cells in a mouse model of limb ischemia. *Proc Natl Acad Sci USA* 106:20399–20404.
57. Sadoun E, Reed MJ (2003) Impaired angiogenesis in aging is associated with alterations in vessel density, matrix composition, inflammatory response, and growth factor expression. *J Histochem Cytochem* 51:1119–1130.
58. Iemitsu M, Maeda S, Jesmin S, Otsuki T, Miyauchi T (2006) Exercise training improves aging-induced downregulation of VEGF angiogenic signaling cascade in hearts. *Am J Physiol Heart Circ Physiol* 291:H1290–H1298.